

Modelling Gravitationally Coupled Modes of High Stellar Mass Protostellar Star-Disk Systems

Aneeq Ahmed

Advisor: Dr. Kathryn Hadley

Submitted July 2017

Table of Contents

Abstract.....	3
Background and Motivation	3
Methods.....	3
Results.....	6
Discussion.....	8
Conclusion.....	12
References	12

Abstract

We computationally modelled protostellar star-disk systems with star to disk mass ratio of 10. Our computational models looked at the development of density perturbations in these systems for different geometries of the system. The ratio of the star's height and radius (r_p/r_e) is varied between 0.1746 and 0.88095. We modelled systems with differentially rotating stars. The results of this research were compared with earlier research done by Hadley *et al.* (2017) to see if there are consistent trends between models with moderate star to disk mass ratio ($M = 4$) and models with high star to disk mass ratio ($M = 10$). A quantity that was considered was β , which is the ratio of the rotational kinetic energy to the gravitational potential energy. Prior research tells us that stellar barlike modes are unstable for values of β greater than 0.274. This was confirmed for the models run in our research. However, unexpected perturbations at the center of the star were also observed in higher modes that were not seen for the $M = 4$ case.

Background and Motivation

While we understand the general picture of star formation in the universe, the specific processes that underlie the formation of stars are not known in depth. Throughout history researchers have attempted to model disks and see how these disks are affected by perturbations. One such contribution was that of Papilizou and Pringle (1984, 1985 and 1987). They were one of the first ones to model thick disks that were differentially rotating. They found that these disks became unstable to perturbations above a threshold. In our research, this threshold (β_{dyn}) is equal to 0.274 for instabilities in barlike modes. The objective of this research is to see if models of high stellar mass ($M = 10$) similarly become unstable over this threshold for barlike modes and to compare our models with research involving lower stellar mass ($M = 4$) models (Hadley *et al.* 2017).

Methods

Introduction

In this section, we talk about the equilibrium and time-evolving models used in our research. In our computational modelling, we keep all parameters except for the height of the star (R_p) constant, so R_p is our variable. A variable R_p means that for each different value of R_p there will be a specific value for the density maximum of star-disk system. The equilibrium method is used to find the log of the density maximum of the system for a specific given geometry and star-disk mass ratio that we are modelling. The time-evolving methods are used

to model the behavior of modes and density perturbations for the system that we have created using the equilibrium methods. The time evolving models are further divided into two types: models obtained from linear methods and models obtained from non-linear methods. We only consider linear time evolving methods in this research, with the hope of modelling these star-disk systems using non-linear time evolving methods in the future. Another important characteristic of the star-disk system is the rotation of the star. Stars can be modelled to rotate with differential rotation or uniform rotation. In this research, we only consider differentially rotating stars.

Equilibrium Method

We looked at the systems with star-disk mass ratio (M) of 10. To find systems with star-disk mass ratio of 10 a series of steps are followed. We input the parameters for the star-disk system we are interested in into the code. We give the program different guesses for the log of the density maximum for the system. Using our guesses, the program constructs models around the given density maximum. We keep using the guesses to narrow down to a value of the density maximum that gives us the system we are looking for; with star-disk mass ratio of 10 and having the geometry we are interested in.

We looked at systems with the central star in differential rotation (DR). The specific angular momentum of the star is given by;

$$h_M(m_{\varpi}) = 2.5 - 2.5 (1 - (m_{\varpi}))^{2/3} \quad [1]$$

Where m_{ϖ} is the cylindrical mass fraction, $\rho(\mathbf{r})$ is the mass density, $Z(\varpi)$ denotes the height of the star at cylindrical radius ϖ .

$$m_{\varpi} = \frac{4\pi \int_0^{\varpi} \varpi d\varpi \int_0^{Z(\varpi)} \rho(\mathbf{r}) dz}{M_*} \quad [2]$$

We assume that the disks rotate on cylinders. The cylinder's rotation is characterized using the power law angular velocity distribution $\Omega(\varpi) = \Omega_o \left(\frac{\varpi}{r_o}\right)^{-q}$, where r_o is the distance on the disk midplane where the density maximum occurs.

The fluid is described using the polytropic relationship $P = K\rho^{1+\frac{1}{n}}$ between density and pressure, where K is the polytropic constant and ρ is the n polytropic index.

The hydrodynamic equations for the inviscid, axisymmetric, steady-state mass and momentum conservation equations are:

$$\nabla \cdot (\rho \mathbf{v}) = 0 \quad [3]$$

$$\rho \mathbf{v} \cdot \nabla \mathbf{v} + \nabla P + \rho \nabla \Phi_g = 0 \quad [4]$$

These equations are solved under the assumptions described above. The fluid velocity is $\mathbf{v} = \Omega(\varpi) \varpi \hat{\phi}$ and the gravitational potential is described by;

$$\nabla^2 \Phi_g = 4\pi G \rho \quad [5]$$

Equilibrium solutions are found by solving the hydrodynamic equations when the time derivative is equal to 0. We keep making guesses for the density maximum of the system until the guessed and calculated structure agree with each other. The resultant solution is what we are looking for.

Linear Time Evolving Method

We use perturbations of the form $A = A_0 + \delta A(\varpi, z, t) e^{im\phi}$ to solve for the linearly unstable modes. A_0 is the equilibrium solution, δA represents the magnitude of the perturbation in the r-z plane and m is the mode of the perturbation. The perturbations and hydrodynamic equations are used to construct the following series of linearized equations (Hadley *et al.* 2017).

$$\partial_t \delta \rho = -im\Omega \delta \rho - \rho_0 \frac{\delta v_\varpi}{\varpi} - \delta v_\varpi \partial_\varpi \rho_0 - \delta v_z \partial_z \rho_0 - \rho_0 (\delta v_\varpi \partial_\varpi + \frac{im}{\varpi} \delta v_\phi + \partial_z \delta v_z$$

$$\partial_t \delta v_z = -im\Omega \delta v_z - \frac{\gamma P_0}{\rho_0^2} \partial_z \delta \rho - (\gamma - 2) \frac{\delta \rho}{\rho_0^2} \partial_z P_0 - \partial_z \delta \Phi$$

$$\partial_t \delta v_\varpi = -im\Omega \delta v_\varpi + 2\Omega \delta v_\phi - \frac{\gamma P_0}{\rho_0^2} \partial_\varpi \delta \rho - (\gamma - 2) \frac{\delta \rho}{\rho_0^2} \partial_\varpi P_0 - \partial_\varpi \delta \Phi$$

$$\partial_t \delta v_\phi = -im\Omega \delta v_\phi + \frac{1}{\varpi} \partial_\varpi (\Omega \varpi^2) \delta v_\varpi - \frac{im}{\varpi} \left(\frac{\gamma P_0}{\rho_0^2} \right) \delta \rho - \frac{im}{\varpi} \delta \Phi$$

We solve the linearized Poisson equation to find the gravitational potential $\Delta\Phi_g$

$$\nabla^2(\delta\Phi e^{im\phi}) = 4\pi G\delta e^{im\phi}$$

The equilibrium solution is perturbed and then is used as the initial condition for the time evolving method. This perturbed equilibrium solution is evolved with time using the linear time evolving methods. These models can be run for three different resolutions 512 x 512, 1024 x 1024 and 2048 x 2048. We only include 512 resolutions models in this paper because models with greater resolution were unable to finish and were taking more than 3-4 months to finish.

3) Results

As mentioned earlier, β is the ratio of the rotational kinetic energy to the gravitational potential energy. The dynamic instability threshold (β_{dyn}) is equal to 0.274 (Hadley *et al.* 2017). When the β of the star is greater than the threshold we expect to observe instabilities in the stellar barlike modes. The systems have star-disk mass ratio $M = 10$, $q = 2$, the ratio of the radius of the disk to the inner edge and the radius of the disk to the outer edge (r_-/r_+) = .58333. For these systems, $r_p/r_e \sim 0.17$ to 0.88, $\beta_* \sim 0.02$ to 0.30 and $\beta_d \sim 0.478$ to 0.497. The β_* of Md is greater than dynamic instability threshold, $\beta_{\text{dyn}} = 0.274$.

Equilibrium Methods

The equilibrium properties of the systems are given in Table 1. ρ_0 is the density maximum of the disk, ρ_c is the density at the center of the star, β_* is the ratio of the rotational kinetic energy to the gravitational potential energy of the star, β_d is the ratio of rotational kinetic energy to the gravitational potential energy of the disk. r_p/r_e is the ratio of the polar radius and equatorial radius of the star, J is the total system angular momentum, J_{rot} is the spin angular momentum of the star, K_d is the polytropic constant for the disk, r_+ is the outer radius of the disk, τ_c is the central rotation period of the star, τ_o is the rotation period of the disk density maximum and r_o is the location of the density maximum in the disk midplane.

	$\log(\rho_0/\rho_c)$	β^*	β_d	r_p/r_e	J	J_{rot}/J	K_d	r_+	τ_c	τ_o	r_o
Md	-2.13	0.30	0.497	0.17	1.62	0.75	1.43	26.9	108.8	580.8	20.4
Mc	-1.75	0.2	0.495	0.37	0.888	0.70	0.611	11.3	45.4	159.7	8.6
Mb	-1.58	0.12	0.490	0.56	0.589	0.64	0.413	7.43	33.4	85.03	5.6
Ma	-1.42	0.02	0.478	0.88	0.296	0.42	0.296	5.05	46.3	48.16	3.8

Table 1: The equilibrium properties of Ma, Mb, Mc and Md are shown

Linear Methods

The results of the linear time evolving models are given in Table 2. Here P_m is the pattern period for the m-th mode, τ_o is the rotation period at the density maximum, τ_m is the rotation period of the m-th mode, ϕ_2 is the gravitational dipole field, ϕ_4 is the gravitational quadrupole field and ϕ_o is the gravitational monopole field.

P_m/τ_o is a measure of how frequently the density distributions of the m-th mode make a rotation in the star-disk system. This quantity is also an eigenvalue of the star-disk model with a given mode. And the constant phase loci plots represent the eigenfunctions of the model. Each model has a unique value for P_m/τ_o and a unique phase plot.

The linear models showed us that for the flattest star (Md) the $m = 2$ is the fastest growing mode while for all the other star-disk systems (Ma, Mb and Mc) $m = 1$ is the mode which grows the fastest. This tell us that above the threshold the star is driving the disk. We know this because $m = 2$ now begins to dominate the system over the threshold and the perturbation being to become unstable. Table 3 shows the order in which the modes are dominant.

	P_1/τ_o	τ_1/τ_o	P_2/τ_o	τ_2/τ_o	P_3/τ_o	τ_3/τ_o	P_4/τ_o	τ_4/τ_o	P_5/τ_o	τ_5/τ_o	ϕ_2/ϕ_o	ϕ_4/ϕ_o
Md	29	0.37	0.53	0.12	0.46	0.25	0.18	0.53	0.67	0.54	- 0.11 716	0.0289
Mc	70	0.54	0.80	0.90	0.27	0.80	0.27	0.78	0.0078	0.84	- 0.11 654	0.0252
Mb	169	0.69	0.37	1.44	0.38	1.25	0.38	1.30	0.38	1.18	- 0.09 872	0.0154
Ma	1.07	0.80	0.91	4.05	0.92	6.97	0.93	9.32	0.94	3.54	- 0.05 295	0.0012

Table 2

	<i>Modes</i> (<i>Most dominant</i> → <i>Least dominant</i>)				
<i>Md</i>	2	3	1	4	5
<i>Mc</i>	1	4	3	5	2
<i>Mb</i>	1	5	3	4	2
<i>Ma</i>	1	5	2	3	4

Table 3

4) Discussion

One Armed Modes (m = 1)

The models in this paper are compared to models run by Hadley et al in earlier research. The star-disk systems modeled by Hadley et al have, $M = 4.00$, $q = 2$, $r_-/r_+ = .58333$ and $r_p/r_e \sim 0.17$ to 0.88 . For these system with moderate stellar mass, $m = 2$ was found to be the fastest growing mode (Hadley *et al.* 2017). However, for the $M = 10$ models found in this paper, the $m = 2$ mode was only the fastest growing for *Md*, the flattest star.

Figure 1 shows the plots of the constant phase loci of the density perturbations for the $m = 1$ modes of the $M = 10$ and $M = 4$ star-disk systems side by side, from the most spherical model to the flattest model. We note that the models for $M = 10$ one armed modes are consistent with the models found by Haldey *et al.* (2017) for $M = 4$ systems. We observe straight density perturbations in the star. The *Ma* model shows a winding arm in the disk which has a phase advance of approximately $\pi/2$. The other models seem to have arms in the disk that start out straight from the inner edge of the disk, advance in phase by π along the points where the density maximum occurs and eventually becomes straight at the outer edge of the disk.

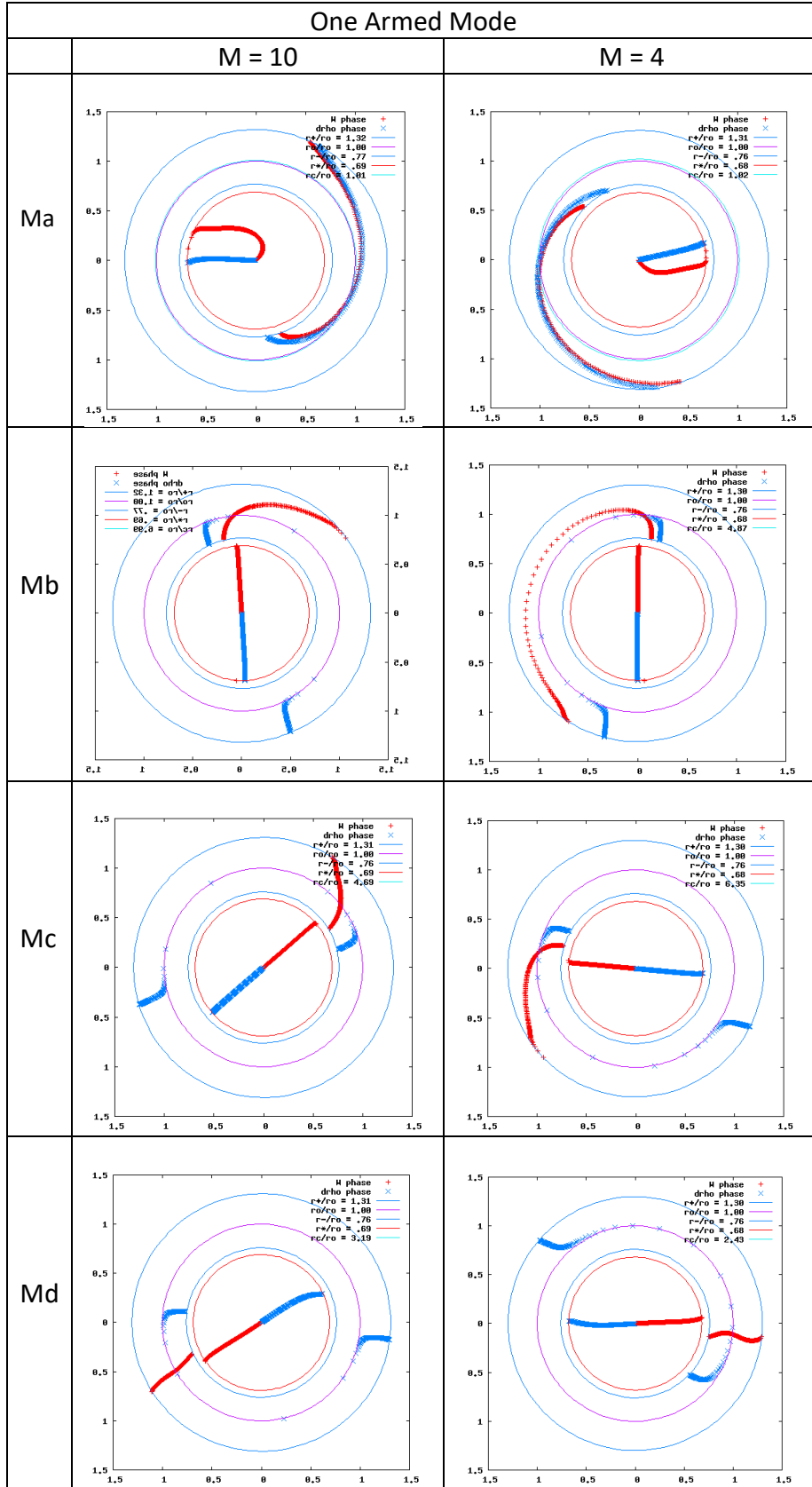


Figure 1: The plots show the constant phase loci $\delta\rho$ (represented by the thick blue lines) in the disk midplane for the $m = 1$ modes of Ma, Mb, Mc and Md. The red circle denotes the stellar equatorial radius, the inner blue circle denotes the inner edge of the disk and the outer blue circle denotes the other edge of the disk

Barlike Modes ($m = 2$)

Figure 2 shows the plots of the constant phase loci of the density perturbations for the $m = 2$ modes of the $M = 10$ and $M = 4$ star-disk systems side by side, from the most spherical model to the flattest model. Comparing the plots for the $m = 2$ case we observe that M_c and M_d are consistent, with M_d having very slightly longer arms in the $M = 4$ model. However, M_a and M_b have models that demonstrate drastically different behavior near the center of the star. The β_* of M_d is greater than dynamic instability threshold, $\beta_{\text{dyn}} = 0.274$. We see that the barlike modes in the star start to become unstable over this threshold and develop winding arms. This agrees with our expectation that unstable barlike modes would be observed over the dynamic instability threshold.

For the M_a case, we see trailing arms in the disks for both $M = 4$ and $M = 10$. But while density perturbation in the star for $M = 4$ is straight, we see winding arms extending from a short straight perturbation in the $M = 10$ case. It is important to note here however that the M_a model was not run until it settled into its modes. The M_a model was run almost 8 times as long as it took for M_b to settle into its modes. We were not able to finish running the M_a model due to time constraints. We hope that further modelling will show if this behavior occurs even after the system settles into its modes.

For the M_b case, we see trailing arms in the disk for both $M = 4$ and $M = 10$. However, these arms are much longer for $M = 10$. They begin in the inner disk and wind around until the outer edge of the disk making a phase advance between 2π and $\frac{3}{4}\pi$. These are much longer compared to shorter arms in the $M = 4$ case which only make a phase advance of around $\pi/2$. These are not the only differences. For $M = 10$, we observe a spiral density perturbation near the center of the star which extends into arms near the midpoint between the center and the edge of the star. These arms straighten out near the edge of the star. The constant phase loci of the density perturbation in the $M = 4$ other hand is a straight barlike mode. This spiral behavior at the center of the star is observed in models with higher modes for $M = 10$. However, none of the modes this behavior occurs in are the fastest growing modes for $M = 10$.

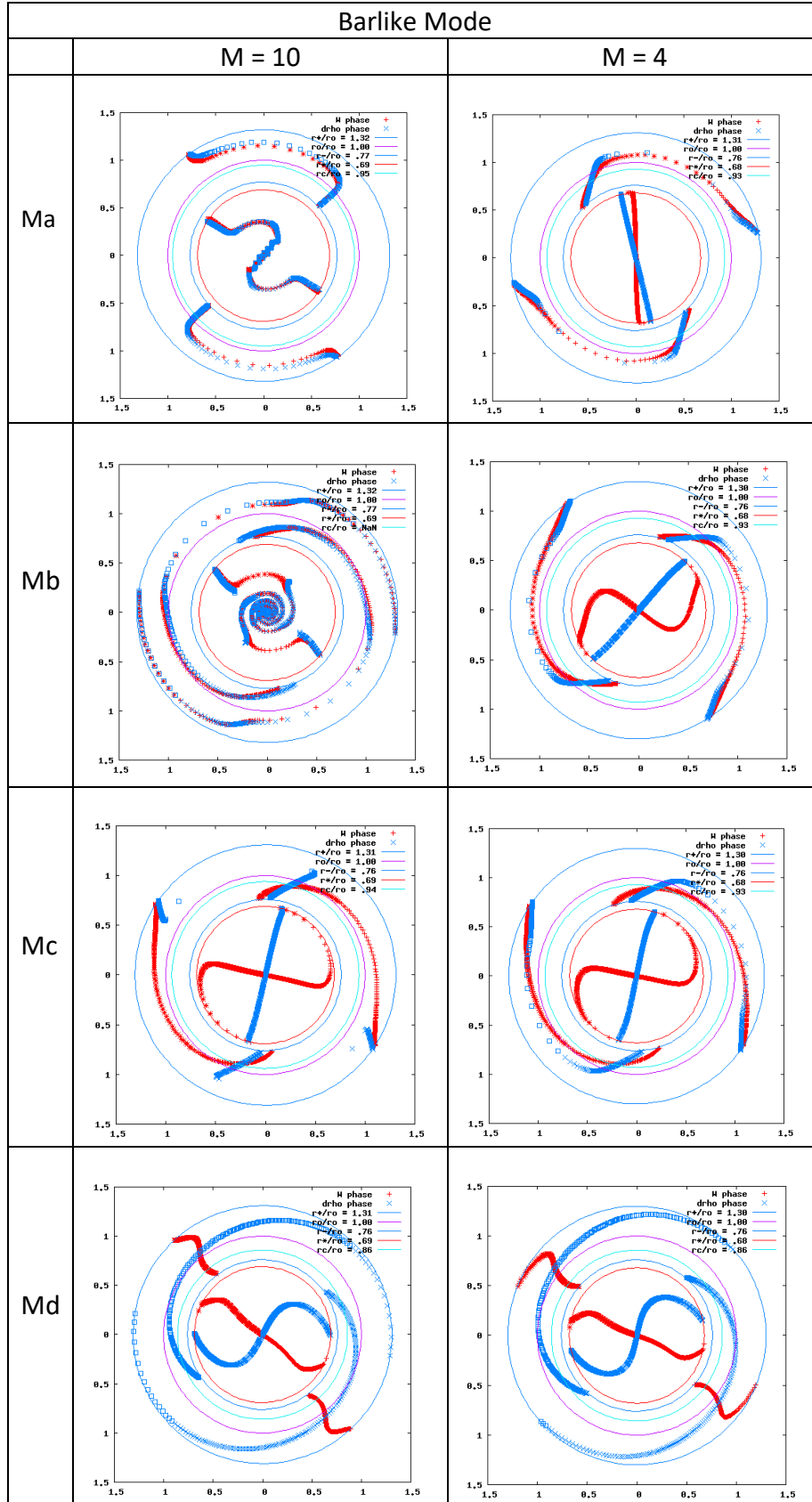


Figure 2: The plots show the constant phase loci $\delta\rho$ (represented by the thick blue lines) in the disk midplane for the $m = 2$ modes of Ma, Mb, Mc and Md. The red circle denotes the stellar equatorial radius, the inner blue circle denotes the inner edge of the disk and the outer blue circle denotes the other edge of the disk

Conclusion

We observe that barlike modes in the stars become unstable for stars with β greater than β_d greater than ~ 0.27 , as reported by Hadley *et al* (2017) in research with star-disk system of star to disk mass ratio (M) of 4. However, we also observe instabilities at the center of stars which are not observed in models with star to disk mass ratio of 4. These instabilities seem to become more common as we look at higher modes. These modes with instabilities at the center grow much slower than the fastest growing modes, and thus they do not have a significant effect on the behavior of the star-disk systems.

In the future, we hope that modelling can be done with systems having star to disk mass ratio different than 10 for higher modes to see if these spiral instabilities at the center of the star occur for other systems. The models run for this paper can also be calculated at higher resolutions of 1024 and 2048 to see if behavior is consistent over a range of resolutions. Modelling using non-linear methods can also be run to gain further insight.

References

- Hadley, K.Z., Fernandez, P., Imamura, J.N., Keever, E., Tumblin, R., & Dumas, W. 2014, *Astrophys. Space Sci.*, 353, 1, 191
- Hadley, K.Z., Imamura, J.N., Keever, E., Tumblin, R., & Dumas, W. 2017, *Astrophys. Space Sci.*, in progress
- Papaloizou, J.C.B. & Pringle, J.E. 1984, *Mon. Not. R. Astron. Soc.*, 208, 721
- Papaloizou, J.C.B. & Pringle, J.E. 1985, *Mon. Not. R. Astron. Soc.*, 213, 799
- Papaloizou, J.C.B. & Pringle, J.E. 1987, *Mon. Not. R. Astron. Soc.*, 225, 267